Theoret. Appl. Mech., Vol.38, No.2, pp. 75–106, Belgrade 2011

Macromolecular structure and viscoelastic response of the organic framework of nacre in *Haliotis rufescens*: a perspective and overview

Jiddu Bezares* **Zhangli Peng†**
Robert J.Asaro‡ **Qiang Zhu§**

Abstract

Nanoindentation probing on nacre obtained from *Haliotis rufescens* shells has demonstrated that nacre displays a combined viscoplastic-viscoelastic time dependent response. Additionally, it is found that the moisture/water content of nacre contributes to its time dependent behavior and overall mechanical properties. Detailed finite element simulations allow for the determination of constitutive parameters used to calibrate specific time dependent material models which are, in turn, compared to those found *via* independent measurement as reported in the literature. The results lead to a new paradigm for nacre's attractive structural composite behavior and thereby to new potential pathways for biomimetics.

Keywords: Mollusk nacre, Viscoelasticity of nacre, Mollusk organic framework

1 Introduction

Nacre, a composite composed of $CaCO_3$ brick-like tiles encased within a biopolymer framework, has long served as a paradigm for biomimetic material design [1] - [7] due, *inter alia*, to its excellent combination of mechanical, structural, and functional biological attributes. For one, the mechanical properties of nacre have long been acknowledged as being extraordinary given the rather

*Department of Structural Engineering, University of California, San Diego, La Jolla, CA 92093

†The same address

‡The same address, e-mail: rasaro@ucsd.edu

§The same address

meager properties of what has been believed to be the ceramic structural component, *viz.* aragonitic $CaCO_3$ [8]-[10]. The structural properties have likewise been routinely cited due to nacre's toughness, with again emphasis given to the fragility of the structural ceramic component, $CaCO_3$. Biologically - and also from the standpoint of materials synthesis - it is noteworthy that nacre is naturally produced from common material constituents, including dissolved calcium and bicarbonate ions, along with a complex biopolymer composed of a chitin core and protein, at completely ambient conditions of temperature and pressure, in sea water [11] - [15]. That is, the processes involving high temperature or pressure, common in the synthesis of ceramic composites, are not involved. In *Haliotis rufescens*, for example, synthesis is mediated by proteins secreted from the abalone's epithelial cells (see *e.g.* [16]-[18]). The detailed structure *vs.* mechanical properties of nacre, however, has as emphviz. the behavior of the biopolymer layers that impart toughness to what would have been thought a rather fragile ceramic composite. Many useful suggestions have been put forth concerning the enhancing yet to be explained due in part to a previous lack of knowledge of the behavior of its constituents, effects of the biopolymer matrix, the nature of the tile's internal structure, and even the possible contributions of "water". A representative selection of them are surveyed in what follows, but as noted below definitive statements and quantification of such effects has yet to be established within these existing reports. Our recent studies have added additional insights to what exists and a more definitive paradigm for why nacre behaves as it does. For example, we provide a quantitative computational model that includes material viscoplastic, viscoelastic and moisture affected composite constitutive behavior. This new perspective will provide guidance for eventual *bioduplication* of enhanced bio-inspired composite materials. Motivation for the present study comes from the recent experimental demonstration of the viscoelasticity of the biopolymer framework by Bezares *et al.* [30]. This work is unique in that it isolated the intact insoluble portions of the biopolymer layers (identified herein as the matrix *interlamellar* layers) and measured and quantified their constitutive response. Specifically what is presented herein is a set of nanoindentation results that document load relaxation caused by the combined viscoplastic response of nacre tiles and the viscoelastic response of the biopolymer matrix. The nanoindentation tests are then modeled *via* a detailed finite element model (FEM) that employs viscoplastic and viscoelastic constitutive models for the nacre tiles and biopolymer matrix, respectively. The constitutive laws and material parameters for all constituents are quantitatively defined. In this important way we attempt to identify the

separate potential effects of biopolymer viscoelasticity and/or moisture content within, and viscoplastic behavior within the tiles. Stiffness values used to calibrate the constitutive models are extracted from the indentation tests, from the measurements of Bezares *et al.* [30], and assessed for consistency *vis-à-vis* literature values. We additionally find that nacre's experimentally observed time dependent response is influenced by its moisture/water content, at least at short times after loading. We find, however, that the effects of moisture/water content in dry nacre appear to be quite modest and are limited to short time loading response. This is vital for an accurate perspective, and is also in contrast to other claims (as noted above) which might well be interpreted to suggest a major influence of "water" content or an influence of undetermined significance. All this leads to a more definitive paradigm, developed and described herein, for nacre's long appreciated attractiveness as a model structural material.

2 Background

Essentially, nacre is a nano-composite composed of layers of aragonite tiles with thickness in the range 250-600 nm sandwiched between biopolymer layers with thickness in the range 20-30 nm (see Fig. 1, *e.g.* [19] - [21], and also [22, 23]). Within each lamella the tiles grow laterally and meet at what becomes polygonal boundaries now commonly called an *intertabular matrix* (see the vertical arrows in Fig. 1 for the location of the intertabular matrix). The tile structure is readily visualized in SEM images as shown in Fig. 1 where the intertabular matrix (*it*) is indicated by the double vertical arrows and the interlamellar layers (*il*) are indicated by single horizontal arrows. The intertabular matrix has been imaged after demineralization by Crenshaw and Ristedt [24, 25] who used histochemical light microscopy to study and map the macromolecular structure within the framework. In this view, the *it* matrix appears as the quasi-hexagonal boundaries of the "imprints" left by the $CaCO_3$ tiles. Bezares *et al.* [27] have additionally shown that the *it*, as well as the *il*, layers contain a structural core comprised of chitin.

Nacre tiles often respond, *via* diffraction, as single crystalline tablets but are known to contain an organic intracrystalline matrix. Recently, for example, Rousseau *et al.* [28] have performed AFM imaging, in tapping mode, and TEM dark field imaging of nacre tablets in the oyster *Pinctada maxima* and provided evidence for a continuous intracrystalline matrix surrounding coherent nanograins that comprise individual tablets. Their results suggest, among

other things, a pathway for modeling the mechanical response of nacre that we use below in suggesting a preliminary model for the tiles themselves. Likewise, Oaki and Imai [5] describe a hierarchical structure of nacre in the pearl oyster *Pinctada fucata* in which individual tiles are seen to be composed of nano-scale "building blocks" (*i.e.* nano-crystals) surrounded by an organic matrix (*i.e.* the intracrystalline matrix). These observations provided additional detail for the existence of organic material within nacre's tiles noted much earlier by Watabe [29].

The AFM images shown by Rousseau *et al.* [28] can be used to demonstrate that the stiffness of individual tiles should be less than that of monolithic $CaCO_3$ and, in fact, just on the basis of a simple rule of mixtures should be on the order of at least 10% less. This estimate is based on the apparent thickness of the intracrystalline matrix as seen, for example, in the phase image of Fig. 3b of Rousseau *et al.* (2005). This fact is used in our modeling described below. At the same time, the intracrystalline matrix would impart increased toughness to the structure *via* the energy absorptive capability of, what is now known to be, a viscoelastic matrix. It is important to realize that attempts to directly probe the constitutive behavior of tiles are complicated by the fact that even nanoindentation involves a composite tile/organic matrix response that must be quantitatively accounted for. This is demonstrated in our computational simulations presented herein which show, *inter alia*, that deformation of the biopolymer interlamellar layers influences the indentation response even for indents as shallow as 50 nm; thus the extracted tile properties depend on those of the *it-il* matrix. Together, the *it* matrix and the *il* layers form a matrix (*viz.* the *it-il* matrix) between and within the aragonite tiles. It is this biopolymer matrix that has been studied by Nudelman *et al.* [26] in *Atrina rigida* and *Nautilus pompilius* and Bezares *et al.* in *Haliotis rufescens* [27] in terms of its macro-molecular structure. Most recently Bezares *et al.* [30] have isolated the *il* layers and measured their viscoelastic constitutive properties as noted above. In the fully hydrated state, Bezares *et al.* [30] fitted the *il* layer response to a standard linear solid model (eq. 4) and found $E_0 = 0.668 \pm 0.088$ GPa, $E_1 = 0.311 \pm 0.092$ GPa, and $\tau = 140 \pm 4$ s. As it happens, we find that intact nacre (*i.e.* nacre within a shell) is well modeled as being viscoelastic as such, but with values of the constitutive parameters being somewhat different as explained below.

There are, as yet, a number of reports describing various aspects of the mechanical behavior of nacre. Most specifically, and relevant to the present work, are those using indentation to probe mechanical response (see *e.g.* [31] - [42],

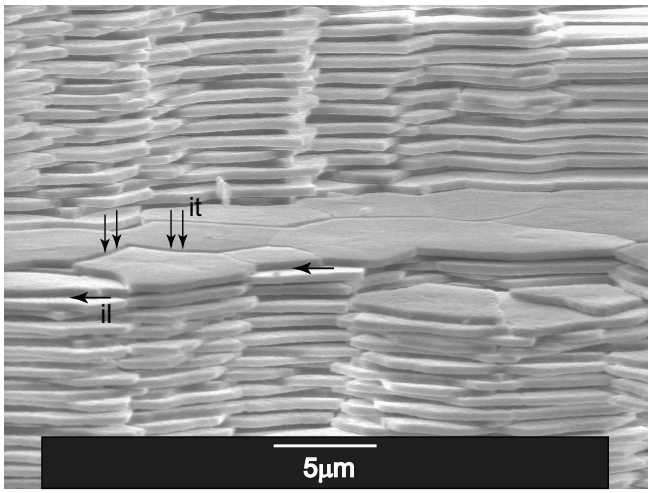

Figure 1: SEM image of a fractured shell section which shows the brick wall like tile structure of nacre. Note the vertical arrows that indicate the intertabular (*it*) matrix between tiles and the horizonal arrow that indicates the interlamellar (*il*) layers.

see also [34] involving a study not involving nanoindentation). Taken together these reports have shed much light on various aspects of the phenomenology of deformation of nacre, while at the same time often presenting conflicting conclusions and perspectives as to the key aspects of nacre that mediate its properties. A brief survey follows.

In an early study Curry [34] conducted studies on the nacre extracted from a variety of gastropods, cephalopods, and bivalves. Curry provided important evidence for inelastic deformation that he described as "plastic", and had also made mention of possible viscoelastic response in the abstract of his paper. However, no particular constitutive models or material parameters were given for this. Moreover, he stated, that some of the response was "anelastic", which of course could mean a response other than a viscoelastic response, but again provided no detail as to the origins or mechanisms of such reversible deformation. Thus important evidence for inelastic and possibly time dependent response was provided by Curry [34] but without any of the constitutive/mechanistic detail required for quantitative analysis, that is, for example as would be needed for numerical model simulations of complete nacre response.

Kearney *et al.* [35] performed nanoindentation on monolithic aragonite and

demonstrated a plastic response. In fact they employed the viscoplastic crystal plasticity model of Peirce *et al.* [49]. They described patterns of pileups around indents and showed that to adequately describe them a crystal plasticity model was required. The precise viscoplastic kinetic parameters were, however, not detailed in their report. The perspective in their report suggests that aragonite is the ceramic constituent of many biological mineralized structures, in particular nacre. Prior to this, Bruet *et al.* [31] performed nanoindentation on nacre obtained from *Trochus niloticus* and found evidence for plastic response of the ceramic tiles. Computational simulations were performed on the composite nacre where the "matrix", *i.e.* the interlamellar layers were modeled as nonlinear elastic (not viscoelastic) and the tiles as essentially aragonite. That is, it was stated "Overall, values obtained from nanoindentation experiments were consistent with macroscopic measurements of aragonite". The precise values of elastic-plastic constitutive parameters were not provided in their report, and no mention was made of viscoplastic behavior. This is in conflict the work of Kearney *et al.* [35]. That aragonite was taken as the model for nacre's tiles was, however, clear.

Huang and Li [32] performed both characterization, *via* x-ray diffraction, and mechanical testing of nacre subjected to heat treatments involving temperatures of up to 1000°C. They report that nacre platelets are composed of nano-sized particles, yet the tiles exhibit single crystal diffraction patterns as noted above. In fact, Barthelat and Espinosa [39], who also describe nacre tiles as composed of nano-crystallites, studied time dependent response of nacre and concluded that nacre displayed a viscoelastic response. No specific model or analysis was presented but they attributed the time dependent response to water content within the nacre structure. It is unlikely, of course, that nacre contains much in the way of a liquid water phase, but rather its moisture content due to various levels of hydration may well influence time dependent response. As far as the ceramic tiles were concerned, Bathelat and Espinosa [39] suggest that monolithic aragonite provides the paradigm - in fact, they state "The results showed that the intracrystalline molecules remaining from the biomineralization of the tablets do not deviate their elasticity significantly from single crystal aragonite." Barthelat *et al.* [41] followed this work with nanoindentation studies on nacre which was modeled as an elastic composite; in fact, the modulus used for the tiles was approximately 80 GPa. In noting the published moduli of monolithic aragonite [44] they stated "This compares very well with the reduced modulus found here (81GPa)". Our results to be presented herein lie in marked contrast to this view and thus provides a rather

different paradigm. Barthelat *et al.* [41] did, however, note that accounting for the influence of the *it-il* matrix (referred to as "interfaces" in their report) was necessary to properly interpret nanoindentation behavior of nacre. They took the *it-il* matrix, however, to be linear elastic. This too is in marked contrast to our paradigm developed below. Likewise Mohanty *et al.* [36] performed AFM tests of the bioploymer layers within nacre and reported a time dependent response that could well be interpreted as viscoelastic. Mohanty *et al.* [36] also base their findings on what are reported to be single protein afm pulling tests. Aside from the fact that the presented force *vs.* displacement curve they present displays major characteristic differences to those reported, and substantiated, for molecules such as titan [45], RNA [48], and spectrin [46, 47], no specific proteins were identified in their work. Moreover, since it is also now known that the structural integrity of the nacre matrix is strongly mediated by its chitin core, it is unclear how relevant such information would be. Chitin does not display such saw tooth like force *vs.* displacement response of a domain unfolding protein like titan or spectrin (see *e.g.* [30]). At least one protein, *viz.* Lustrin A, that contains a foldable domain structure has been isolated from the organic matrix of nacre [38]. However, the report of the afm pulling experiments of Mohanty *et al.* [36] does not mention how, or if, this protein was isolated and/or selectively adhered to. Again, it is vital to understand that since the structural integrity of nacre's organic matrix is due to its chitin network, it is unlikely that the isolated response of a protein such as Lustrin A would be relevant with respect to the overall mechanical response of nacre *per se*. What can be said is that evidence for time dependent response was found but its causes, *e.g.* viscoplastic response of the tiles, viscoelastic response of the matrix, moisture content in the biopolymer matrix, and full characterization remained unclear. AFM molecular pulling experiments have been performed by others, *e.g.* Smith *et al.* [43], on material lying within the organic matrix of nacre from Haliotis rufescens. Their emphasis, however, was more on the role of proteins in contributing to adhesion, clearly of importance *vis-à-vis* the composite's internal binding.

Taken together, the general view outlined to date is that nacre is composed of a layered brick-like tiled structure encased within a bioploymer matrix. The "bricks", or tiles, are themselves nano-scale composites composed of crystallographically aligned nano-sized grains separated by a biopolymer matrix. The aragonite ceramic within the tiles displays a plastic response, and presumably viscoplastic. Here we add the note that this nanocrystalline (and textured) tile structure is already significantly toughened as compared to monolithic arago-

nite due to its nano-scale grain structure and tough biopolymer matrix. This perspective has also been given by Li *et al.* [42] with respect to toughness, but they provided no constitutive description of nacre tiles that may be used for either analysis or confirmation, for example confirmation obtained *via* comparisons between experiment and model simulation. Their emphasis was instead on mechanisms such as micro-crack deflection within and about the nanograins known to be characteristic of nacre tiles [5, 28] and crack blunting due to the also known plasticity of aragonite, both being important mechanisms imparting toughness. The role of an intra-tablet biopolymer matrix was not specifically considered. Thus, although there have been repeated claims that the response of nacre tiles is unaffected by the biopolymer structure within them, we find that the ceramic/bioploymer composite tiles cannot be effectively modeled using the properties of monolithic aragonite. The *il-it* matrix is known to be viscoelastic (with a tensile strain to failure exceeding 3-4%) based on the recent findings of Bezares *et al.* [30]. What our findings also suggest is that nacre's moisture/water content also contributes to its time dependent response and thus the biopolymer matrix may be potentially viewed as behaving also as a dense sponge-like medium, and thus energy absorptive. What is then required is a way of identifying, and sorting out, the effects of the various potential contributions to the overall viscoelastic/viscoplastic behavior.

Our essential focus is on correlating the behavior of nacre in intact shells that have been removed from an aqueous environment. Such nacre is referred to as *dry nacre*. To gain additional perspective, however, tests were performed on nacre that was hydrated by emersion in water for extended periods of time as detailed below - this is referred to in what follows as *wet nacre*. Moreover, nacre subjected to heat treatment at elevated temperatures sufficiently high as to remove the *it* and *il* layers was tested also as described below. Our detailed FEM analysis is focused on *dry nacre* as we find that this leads to more definitive results when compared to experiment. In wet nacre the behavior was found to be extremely sensitive to the precise conditions of hydration (*e.g.* to the duration of hydration) which made definitive property characterization challenging. Establishing the full effects of hydration, therefore, would require an additional focused study.

In the next section we describe the sample preparation, the nanoindentation methods used, and the finite element models employed in this study. It is followed by the presentation of experimental results. These results are duplicated numerically, from which the constitutive properties of the structural components are extracted and the detailed responses of these components are

predicted. Based on these we propose a model explaining the origins of the viscoelasticity of the system and a new paradigm for potential synthesis of bio-duplicated composites in the Conclusions and Discussion.

3 Materials and methods

3.1 Nacre and aragonite specimens

Fresh shells from *H. rufescens* were obtained from the Abalone Farm Inc. in Cayucos, CA. The nacre extracted from these shells contained no interlayers and was thus judged to a high quality nacre suitable allowing unambiguous assessments of the behavior of nacre. These were washed and stored dry at 4°C. Strips of shell were cut out using a cutoff wheel and split along their thickness using a hammer. During fragmentation thin translucent nacre flakes were released. The thinnest flakes were inspected under an optical microscope where individual tiles could be resolved. Flat regions containing planes with hundreds of tiles and few defects were identified and selected for indentation tests. Flakes were glued to AFM pucks and tested as described in the following section. An aragonite crystal was purchased from a mineral supplier in Encinitas, CA. The crystal was sectioned using a SiC cutoff wheel, polished using standard metallographic procedures, and etched for 5min in 0.5M EDTA pH8.0. Crystal sections were mounted on AFM pucks for placement and alignment in the nanoindenter.

Heat treated nacre samples were prepared by mounting nacre sections on AFM pucks and were then placed in an oven, in air, for 12 hours at 200°C. Hydrated nacre samples were placed in dI water for 3 days prior to testing. The samples were maintained moist during testing.

3.2 Nanoindentation

A Ubi 1 Nanomechanical test instrument (Hysitron, Inc., Minneapolis MN) with a diamond Berkovich tip having a 100 nm radius of curvature, was used for all tests. A trapezoidal load function with a 5 second hold under load-control was used to determine the elastic modulus for contact depths ranging between 25 nm and 300 nm. The Young's modulus was determined from the load (P) *vs.* indentation depth (δ) curves using the method described by Oliver and Pharr [50]. In this approach, the reduced modulus E_r is first determined from the slope of the initial part of the unloading curve and the area of elastic contact. It is then related to the Poisson's ratio ν and the Young's modulus

E_0 of the specimen by

$$1/E_r = \left(1-\nu^2\right)/E_0 + \left(1-\nu_i^2\right)/E_i, \tag{1}$$

where $\nu_i = 0.07$ and $E_i = 1141$ GPa are the Poisson's ratio and the Young's modulus of the diamond indenter, respectively. We assume that the Poisson's ratio of the nacre tiles is $\nu = 0.3$, a typical value for crystals undergoing plastic deformation.

Figure 2 shows P *vs.* δ results used to determine properties such as modulus and hardness. Displacement controlled relaxation tests were performed using a trapezoidal load function with a 40 second hold and a maximum displacement of 75 nm. Drift was monitored for 40 seconds before performing each indent, and the displacement was held for 180 seconds between tests to allow the system to stabilize. All tests were performed at room temperature in an isolation chamber.

3.3 Simulation and analysis

3.3.1 Finite element models

A finite element method was developed using ABAQUS Explicit (ABAQUS Inc., Providence, RI) to simulate the time dependent processes associated with nanoindentation of nacre. For computational efficiency, the symmetry of both the Berkovich indenter and an idealized mineral tile were exploited and only 1/6 of the system was modeled (Fig. 3). Surface A is allowed to slide tangentially due to the weak constraints from surrounding tiles and inter-tablet biopolymers. No displacement is allowed at the bottom. Other boundary conditions are specified based on the symmetry described in Fig. 3.

To make sure that our computational domain in the thickness direction (along the C-axis) is sufficiently large (*i.e.* there are enough layers included in the simulation so that the no-displacement boundary condition at the bottom is sufficiently accurate), numerical tests were undertaken to ensure that during the indentation simulation the deformation of the layers far from the indenter was negligible. In practice we found that this was achieved by using five mineral tile layers and five biopolymer layers (Fig. 3). Near the contact region, the computational mesh was significantly refined for high resolution; overall we use 167228 C3H8R elements (*i.e.* uniformly reduced integration brick element). The Berkovich indenter is modeled as a rigid surface with inclined face angle β of 24.7° and apex angle γ of 77.1°. The mineral tiles were idealized as perfect hexagons with edge length of 2.5 μm and thickness of 600 nm. The thickness

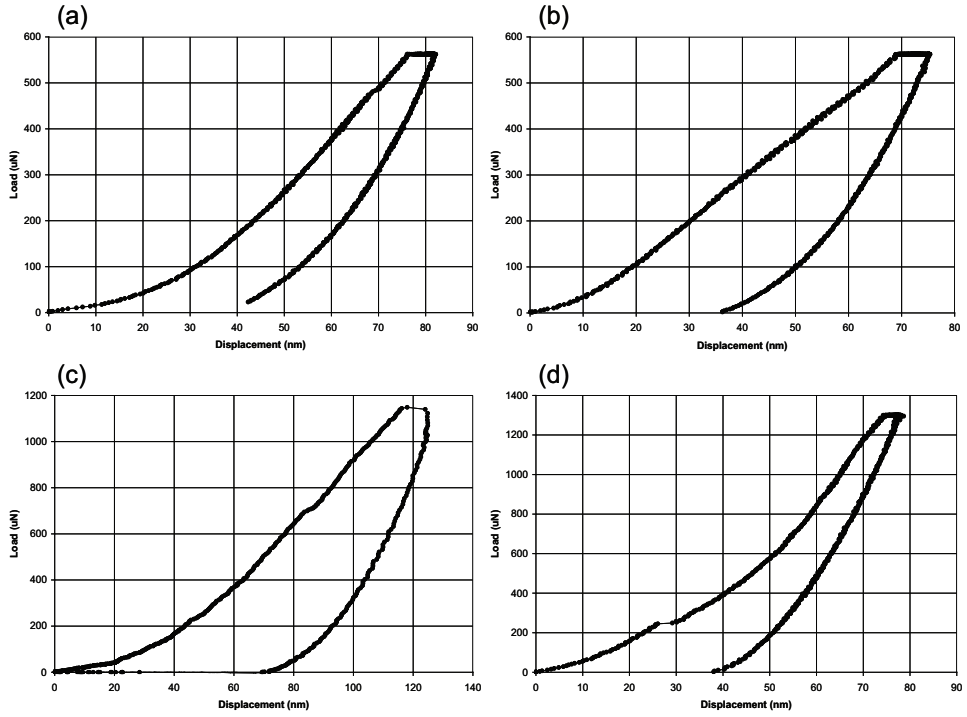

Figure 2: Typical load-displacement curves for (a) dry nacre, (b) heat treated nacre, (c) wet nacre, and (d) monolithic aragonite; note the load plateau at loads $\sim 230\mu$N.

of the biopolymer layers is 20 nm. These parameters are all based upon our experimental measurements. The interaction between the indenter and the nacre was considered as a hard contact without friction.

A similar finite element model was developed to extract viscoplastic properties from the indentation relaxation experiments on monolithic aragonite. This model involved the same mesh as the one used for the nacre (Fig. 3), whereas the biopolymer layers were replaced by aragonite. Furthermore, in this monolithic aragonite model surface A was fixed in all directions due to the strong constraints from surrounding minerals.

3.3.2 Constitutive relations

Both the aragonite tiles and the monolithic aragonite were considered as viscoplastic materials, whose constitutive properties were modeled using the rate-

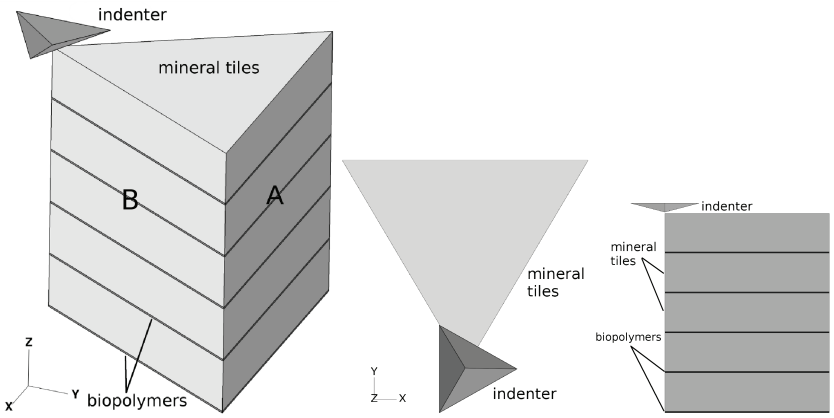

Figure 3: The finite element model of the nanoindentation process: 3D view (left), top view (middle), and B section view (right).

dependent plasticity overstress model by Perzyna [51], *i.e.*

$$\dot{\bar{\varepsilon}}_p = \frac{\sigma_Y}{\eta_p}\langle\frac{\sigma}{\sigma_Y} - 1\rangle^n, \tag{2}$$

where $\dot{\bar{\varepsilon}}_p$ is the equivalent plastic strain rate, n is the rate-sensitivity exponent, σ_Y is the yield stress, η_p is the plastic viscosity, and σ is the Cauchy stress. Plastic straining happens when the yield condition $\sigma > \sigma_Y$ is satisfied, which is incorporated *via* the Macaulay bracket $\langle\rangle$ ($\langle f\rangle = f$ if $f > 0$, and $\langle f\rangle = 0$ if $f \leqslant 0$). For simplicity, the rate-sensitivity exponent n was set to unity so that Eq. (2) becomes

$$\dot{\bar{\varepsilon}}_p = \frac{\langle\sigma - \sigma_Y\rangle}{\eta_p}. \tag{3}$$

We note that setting $n = 1$ in Eq. (2) led to results that matched experiments quite closely, as will be shown below, and thus we used that value consistently as in Eq. (3).

For the biopolymer layer, a standard linear solid model of viscoelasticity is used (as shown in Fig. 4). We have

$$\sigma = \int_0^t E(t - t')\frac{de}{dt'}dt', \tag{4}$$

where $E(t) = E_0 + E_1 \exp(-t/\tau)$ is the instantaneous Young's modulus, E_0 is the Young's modulus, $\tau = \eta/E_1$ is the characteristic time, η is the viscosity, σ is the Cauchy stress, and e is the engineering strain.

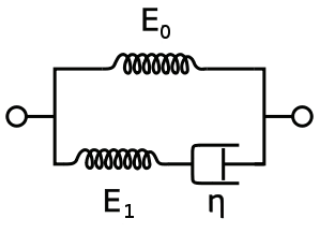

Figure 4: The standard linear solid model.

4 Results

4.1 Nanoindentation tests

4.1.1 Indentation profiles

Typical indentation profiles are shown in Fig. 5. Figure 5a shows a typical scan of an indent performed on *dry nacre* (*i.e.* nacre not submersed in water for any extended period of time prior to testing). Pileups are clearly visible surrounding the indentation that are symmetrical unlike those shown by, for example, Kearney *et al.* [35] who studied monolithic aragonite. Rather the pileups are more characteristic of those expected to result from indenting an isotropic elastic-plastic material (see *e.g.* Mulford *et al.* [52] who performed microindentation on pure Cu). Figure 5b shows an indentation profile for hydrated (or *wet*) nacre - in these cases the form of the indentation was different in that the pileups are far more "blunted". These pileups are, in fact, similar to those showed by Mulford *et al.* [52] in ductile materials like pure polycrystalline Cu. Scans of the indentation profiles made on heat treated nacre do not resemble both the dry and the wet cases (Figure 5c). In such cases the indents appeared to have sharp edges and displayed no pileups *per se*. In fact, they are reminiscent of an indent made on a loosely compacted granular material such as an unsaturated porous sand.

The indentation profiles on monolithic aragonite displayed anisotropic pileups similar in appearance to those reported by Kearney *et al.* [35] as seen in Fig. 5d. This is indeed expected for an indentation made on an anisotropic elastic-plastic material such as ductile crystal. It has also been analytically confirmed by Kearney *et al.* [35] using a crystal plasticity theory such as outlined by Asaro and Lubarda [53]. These results suggest that: 1) nacre behaves as a viscoplastic solid but, unlike monolithic aragonite, is more isotropic and unlike an anisotropic single crystal; 2) after heat treating, and with the con-

comitant loss in intra-tile protein, nacre behaves as a loosely bound granular material; and 3) in a fully hydrated state, *i.e.* with extended exposure to water, nacre again behaves as an isotropic viscoplastic solid, but with a much reduced hardness as compared to *dry nacre*. This is discussed further below.

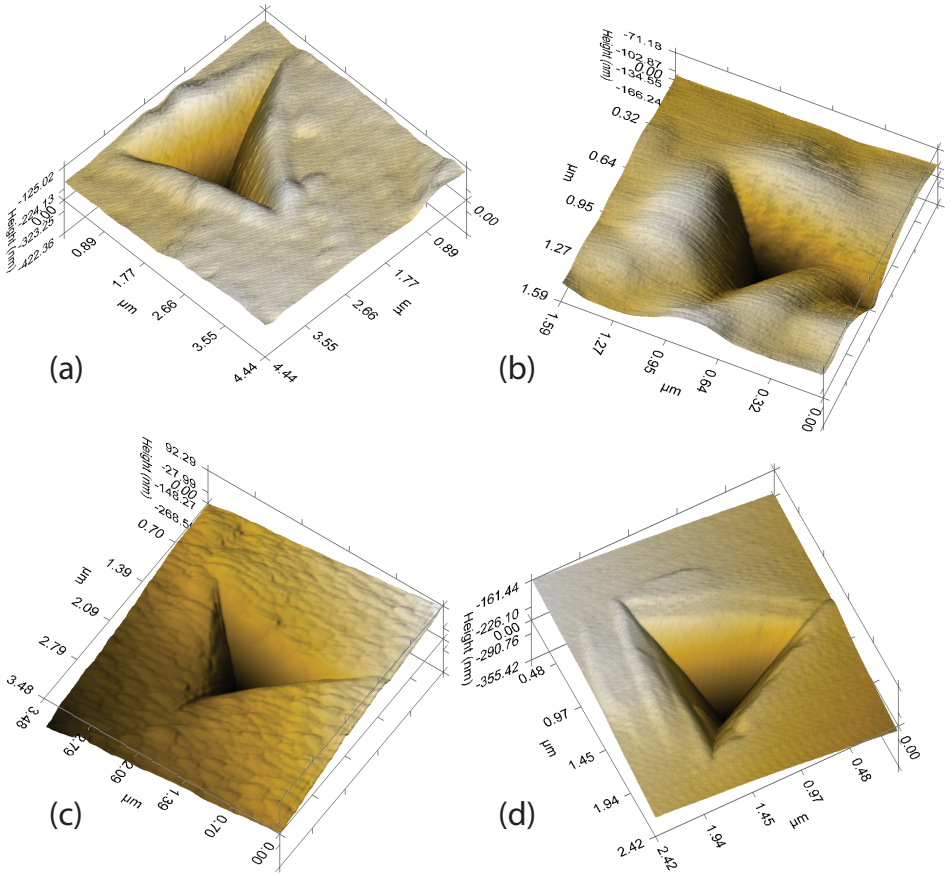

Figure 5: Indentation profiles on: (a) dry nacre. There are pileups around edges; (b) wet nacre. The blunted appearance of the indentation is related to the compliance of the wet nacre seen from its relatively low modulus; (c) heat treated nacre. The material appears compacted and similar to what happens to sand when it is heated and grains begin to fuse together; and (d) monolithic aragonite. The uneven pileup indicates anisotropy. A slip band is also visible on the left face of the indent associated with load plateaus in the P-δ curves.

4.1.2 Young's modulus

Values of 70, 80, and 100 GPa have been used in previous models of nacre as the Young's modulus of the biomineral by for example Wang *et al.* [54], Barthelat *et al.* [40], and Gao *et al.* [8] respectively. We note that the out-of-plane modulus of nacre tiles is not the same as that of monolithic aragonite along its c-axis due in part to protein embedded within the tiles. Furthermore, the Young's modulus of nacre, as determined from nanoindentation tests, varies with indentation depth. With increasing depth, there is an initial exponential decrease in modulus, followed by an eventual taper to a constant value. In monolithic aragonite the modulus begins to taper at ∼300 nm, eventually reaching a constant value of ∼80 GPa. Fig. 6 shows the variation in the reduced modulus of aragonite, *dry nacre*, heat treated nacre, and *wet nacre*, up to indentation depths of 300 nm. In our following finite element simulations, Young's modulus of aragonite crystal at a 55 nm indentation depth was derived from such indentation experiments performed to the same depth.

We perform simulations of 55 nm deep indentations in aragonite crystal along its c-axis and 75 nm indentations in dry nacre along the out-of-plane direction of a single tile. As seen in Fig. 6, the Young's moduli in these two cases are around 114 GPa and 70 GPa, respectively. The Young's modulus of single tiles, which contain protein inclusions, falls between those of nacre and monolithic aragonite. Biopolymer layers in nacre make it more compliant than single tiles. The tiles however contain protein inclusions not found in aragonite, thus they are more compliant than the monolithic crystal. Sterographic measurements from SEM images of deproteinized as well as heat treated nacre indicate the void fraction in single tiles to be approximately 20%. Thus the modulus of a single tile is taken as 90 GPa, which is a 20% reduction in the modulus of aragonite.

We note, in particular, that scatter in the graph for wet (*i.e.* hydrated) nacre is too great for accurate determination of the modulus. This is probably due to the complicated and inhomogeneous structure of the biomineral tablets, which contain protein inclusions that undoubtedly swell after hydration, leading to the softening of the mineral.

4.1.3 Load relaxation

Drift was checked on fused quartz and monolithic aragonite standards, whereby it was found that a displacement overshoot during loading resulted in an initial rapid decrease in load within the first 3 seconds of the tests such as shown in

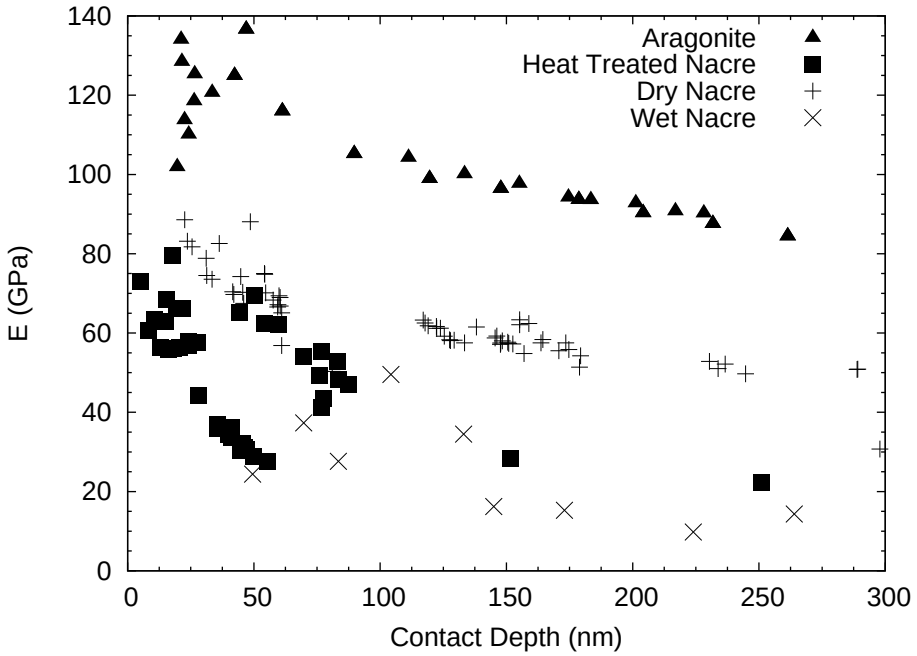

Figure 6: Young's modulus *vs.* indentation depth for monolithic aragonite, heat treated nacre, dry nacre, and wet nacre.

Fig. 7. Results from this initial period were thus excluded from the analysis. The viscoplastic behavior of the biomineral tablets in nacre was tested in comparison to viscoplastic behavior seen in monolithic aragonite. Relaxation tests performed on monolithic aragonite showed that the mineral exhibits a long-term viscoplastic response to indentation loading as seen in Fig. 7. The effect of the biopolymer layers on time-dependent behavior is clear in this figure, where relaxation is pronounced in *dry nacre*, even more so in *wet nacre* and significantly less in heat treated nacre. Recovery tests were performed to verify that the long-term behavior was not due to drift. Linear drift was monitored and was less than 1 nm/s. The implications of these results are discussed next where we present results from our numerical simulations.

4.2 Numerical simulations

Finite element simulations were performed for indentations on monolithic aragonite and *dry nacre* as noted in the Introduction. Particular attention was paid

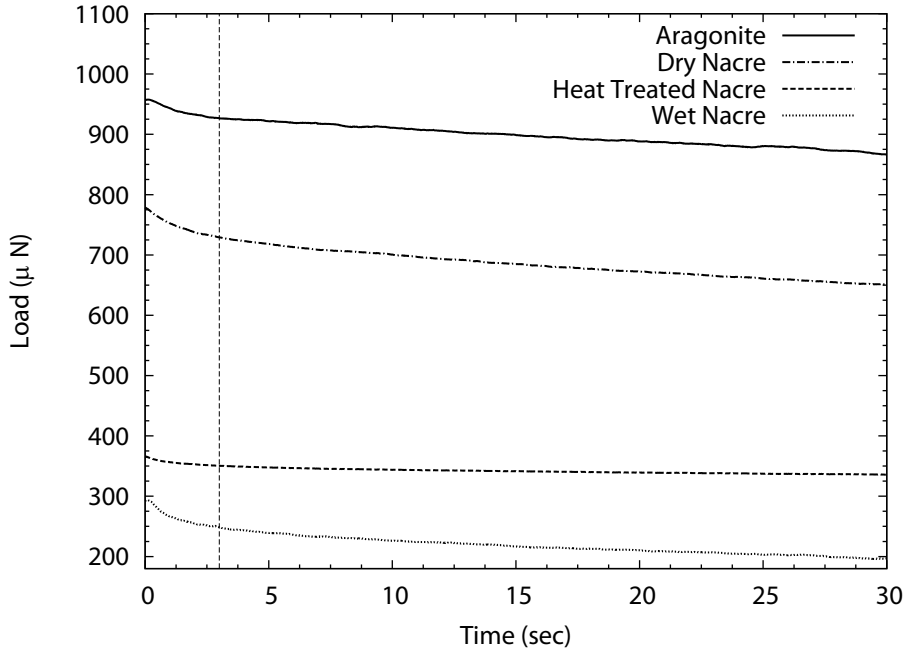

Figure 7: Relaxation curves for monolithic aragonite, heat treated nacre, *dry nacre*, and *wet nacre*. Note the greater amount of relaxation observed in *wet nacre* and the nearly absent relaxation observed in heat treated nacre.

to comparison with the experimentally obtained load relaxation records. For this purpose, it was found that both viscoplastic and viscoelastic parameters were needed for accurate fitting of the time dependent responses.

By numerically duplicating the relaxation curves of the monolithic aragonite using our finite element model (Fig. 3), we estimated that the Young's modulus of the monolithic aragonite $E_{aragonite} \approx 114$ GPa, the yield stress $\sigma_Y \approx 10$ GPa, and the plastic viscosity $\eta_p \approx 5000$ GPa·s.

Similarly, we carried out simulations for indentation on *dry nacre*. Since the mineral tiles of nacre include a certain amount of biopolymer (Bezares *et al.* [30]), they are expected to be more compliant than monolithic aragonite. Based on SEM images, we estimate that the inclusion ratio of the mineral tiles is about 80% so that the stiffness reduction is around by 20%; in the following simulations we choose the Young's modulus $E_{tile} \approx 90$ GPa, the yield stress $\sigma_Y \approx 8$ GPa, the Poisson's ratio $\nu = 0.3$, and the plastic viscosity $\eta_p = 5000$ GPa·s.

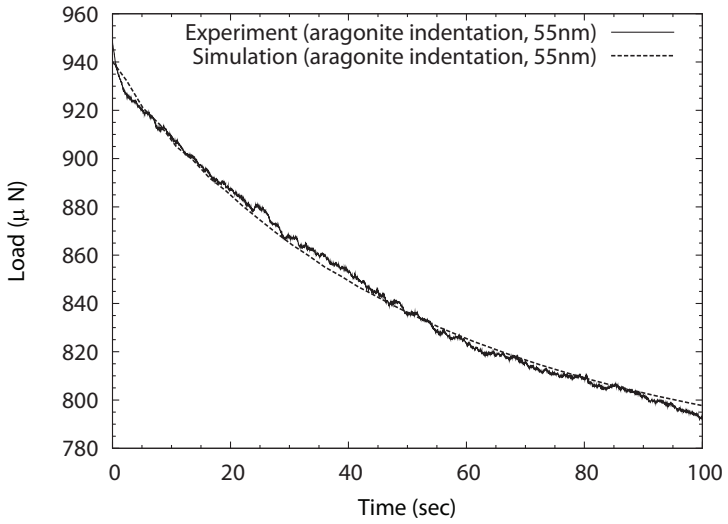

Figure 8: FEM simulation of the monolithic aragonite indentation relaxation. The indentation depth is 55 nm.

Close inspection of the relaxation curves of *dry nacre* show that there is a short term viscoelastic behavior with a characteristic time of approximately 1 second, and a long term viscoelastic behavior with a characteristic time of around 50 seconds. The speculation is that the short term viscoelastic behavior is attributed to the sudden drainage of the water in the biopolymer layers, whereas the long term viscoelastic behavior is due to deformation of the biopolymer itself. To identify the short term and long term viscoelastic properties of the biopolymer, we carried out a short simulation with $E_0 = 0.1$ GPa, $E_1 = 0.88$ GPa, $\tau = 0.7$ s (Fig. 9) and a long simulation with $E_0 = 0.015$ GPa, $E_1 = 0.135$ GPa, $\tau = 45$ s (Fig. 10). In both cases we assume $\nu = 0.3$. With these parameters, both the short time and the longer time responses are accurately reproduced. This further leads us to propose a novel paradigm for the nacre composite discussed in the Discussion and Conclusions section.

Our results show that the biopolymer layers (especially the one nearest the indented surface) contribute significantly to the overall deformability of the nacre during indentation. For example, by considering a case with an indentation depth of 75 nm (by using the set of parameters in the long simulation), it was found that the maximum thickness changes of the first mineral tile and the first biopolymer layer are 49.1 nm and 11.6 nm, respectively. The total thickness change of all other layers was 14.3 nm. In Fig. 11 we plot contours of

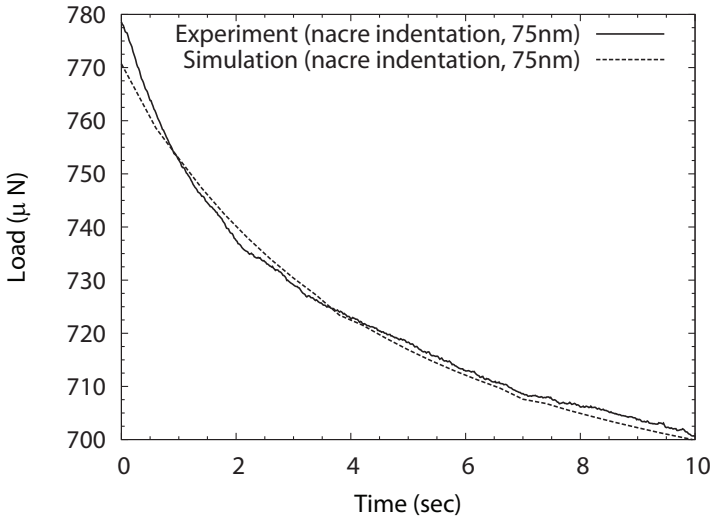

Figure 9: A short-term simulation of nacre indentation relaxation. The depth of indentation is 75 nm.

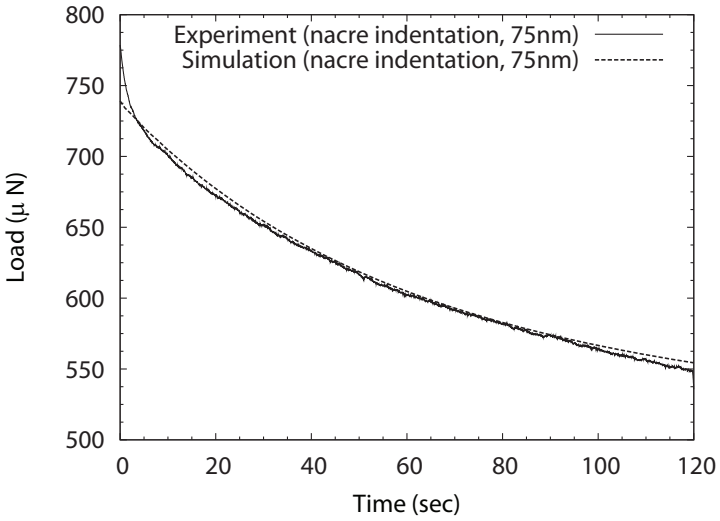

Figure 10: A long-term simulation of nacre indentation relaxation. The depth of indentation is 75 nm.

the logarithmic strains e_{33} (in the thickness direction) and e_{11} (in-plane strain). e_{33} displays a large negative value (-0.87) at the first biopolymer layer, sug-

gesting that the nacre was significantly compressed in that area. Figure 11b shows that the first biopolymer layer is also slightly stretched ($e_{11} > 0$), but its strain e_{11} is much smaller than e_{33}. In the second biopolymer layer, e_{11} was significantly decreased.

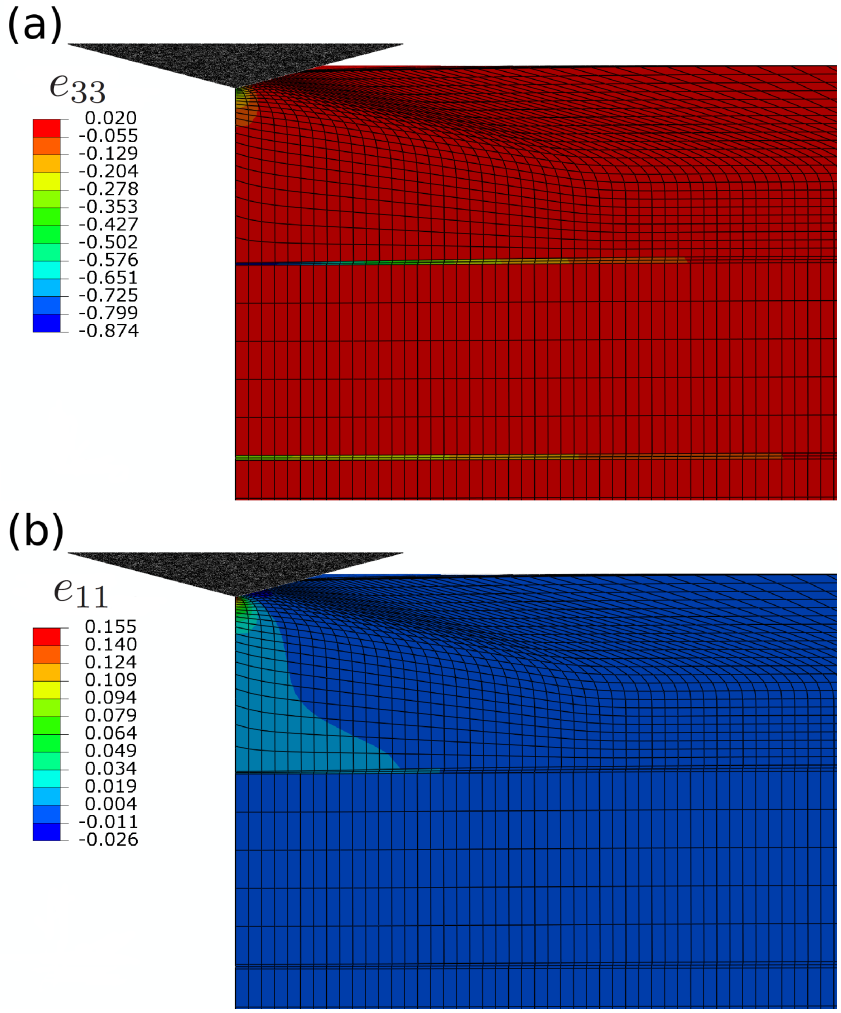

Figure 11: Contours of (a) strain e_{33} and (b) strain e_{11} of nacre indentation (B section view). The indentation depth is 75 nm.

For both monolithic aragonite and nacre indentations, our finite element simulations underestimated the experimentally observed height of the pileup.

This characteristic is consistent with other numerical models (*e.g.* Bruet *et al.* [31]). It, however, does not have a significant effect on the accuracy of our prediction of nacre viscoelasticity. Incidently, the detailed pileup geometry of monolithic aragonite can be more accurately simulated through a crystal plasticity constitutive model developed by Kearney *et al.* [35]. Such detail was not a focus of the present study.

5 Discussion and conclusions

Our results have provided evidence for the general picture of nacre's constituency, and have shed new light on the relationship between its makeup and its performance as a structural composite material. Based upon these findings, it is useful to propose a novel model, or paradigm, for such a layered composite as shown in Fig. 12. Toughness is obtained firstly by virtue of the large tile aspect ratio, *viz.* a tile diameter/thickness ratio that lies in the range 10-20, (*e.g.* Gao *et al.* [8, 9]), and by the fact that the interdigitated brick-like tile layers are encased within a soft, ductile biopolymer matrix. The large tile aspect ratio provides efficient load transfer and the biopolymer layers provide, *inter alia*, for crack deflection mechanisms. Moreover, the tiles themselves are not fragile monolithic $CaCO_3$, but are actually nanocrystalline with embedded proteinaceous material, as indicated in the tile drawn at the upper left corner of Fig. 12b. Thus the tiles themselves are toughened ceramics with a stiffness and hardness clearly reduced as compared to those of monolithic aragonite. As noted in the background discussion, there has been considerable suggestion that monolithic aragonite can serve as a model for nacre tiles. Our results suggest quite the contrary, from the standpoints of elastic and viscoplastic response, and fracture resistance, *inter alia*. The biopolymer matrix is viscoelastic and is characterized by a large elongation to failure ($> 3\%$) as demonstrated by Bezares *et al.* [30]. Still another feature of nacre is its moisture/water content, also indicated in Fig. 12. This provides an additional contribution to the overall time dependent constitutive response of nacre and for still another mechanism of energy dissipation during deformation. We fall short of suggesting that the biopolymer layers of nacre behave as a tough sponge *per se*, since the water, *i.e.* moisture, content of the *it* and *il* layers is undoubtedly low; thus describing the moisture effects to a liquid water phase *per se* is most likely misleading. Yet we believe that the presence of moisture/water within those layers does indeed provide for an additional energy dissipative mechanism that contributes substantially to nacre's toughness. This apparently has yet to be

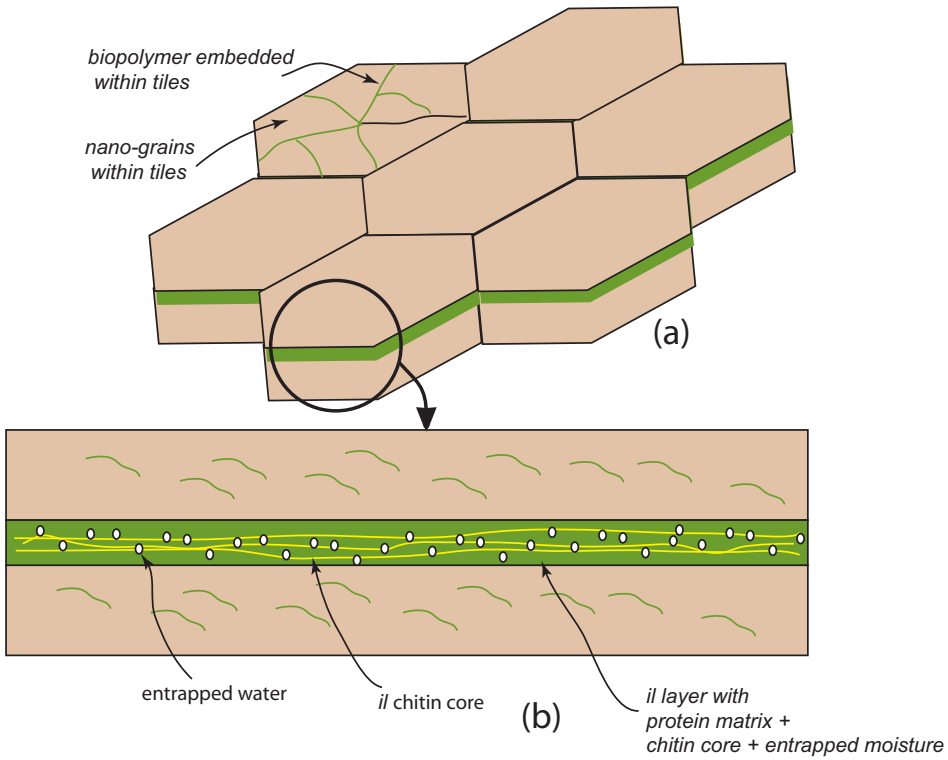

Figure 12: Paradigm for the structure and performance of nacre. (a) Brick-like layered tile composite composed of high aspect ratio toughened ceramic $CaCO_3$ tiles within a biopolymer matrix; (b) the biopolymer matrix, which is itself viscoelastic, is composed of a chitin core within a hydrated protein matrix. Note that the tiles are themselves toughened by the incorporation of an intra-tile biopolymer network.

quantified in the literature.

The paradigm depicted in Fig. 12 is intended to provide a basis for developing new pathways for biomimetics, *i.e.* for bio-duplication of novel synthetic composite materials. A key to this would be to sandwich high aspect ratio toughened ceramic tiles with moisture/water containing viscoelastic tissue (*e.g* polymer). Perhaps not emphasized in the literature, to date, it is required as shown herein that the ceramic tiles themselves need be toughened. Monolithic $CaCO_3$ ceramic tiles in nacre would not have produced a composite with the attractive strength-toughness properties now well attributed to naturally

synthesized nacre.

Our studies of heat treated nacre have provided additional perspective on the vital role of the biopolymer framework with respect to the mechanical performance of nacre. Firstly, indentation on heat treated nacre clearly showed the structure of nano-sized grains within each tile as displayed in Fig. 13a, for example. Several nano-grains are indicated by arrows. The material still appears compacted after heat treatment even with the polymer content removed. The general appearance is similar to that of sand as it is heated and grains begin to fuse together. Furthermore, we note that no pileups are visible around the edges of the indentations as is evident in Figs. 13b and 5c.

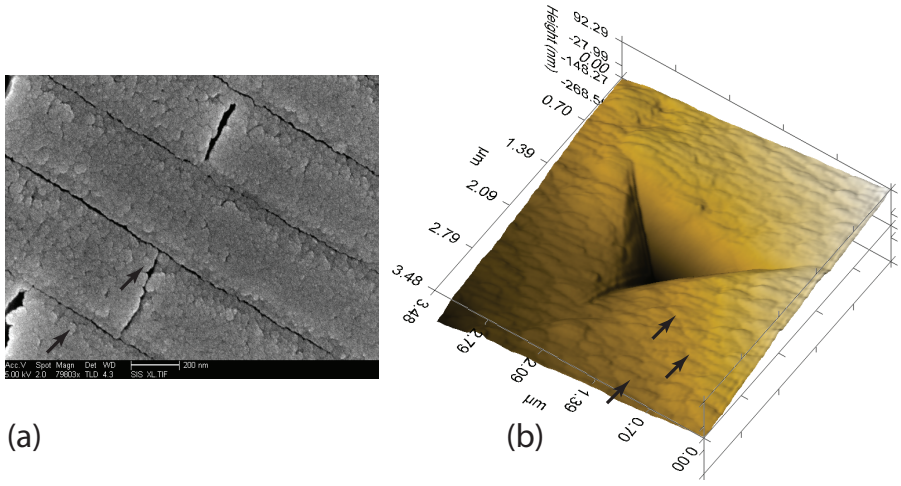

Figure 13: Heat treated nacre. (a) SEM image of a cross section of heat treated nacre. Note that the nanocrystalline nature of the tiles is made evident by the removal of the protein content of each tile. Arrows point to examples of nanocrystals within each tile. (b) Scan of a typical indent made on heat treated nacre (again see arrows that point to nanocrystals). Note the absence of piling up as discussed in the text.

After heat treatment, not only is the protein in the *it* layers and *il* layers burnt off, but the protein inclusion within the mineral tablets is also removed. For example, from Fig. 14a it is clear that what remains are $CaCO_3$ tablets that are porous wherein both the *il* and *it* layers are removed. The removal of the *it* matrix is indicated by the white arrows in the figure. Thus the reduction in Young's modulus of nacre, following heat treatment, can be explained from the above observations, as being due to the degradation of the organic framework

between the tiles, across which load is typically transferred. Heat treatment is also seen to reduce the toughness of nacre at the scales of both the bulk material and the individual tiles. At the scale of the shell, fracture can easily be achieved by the application of a small load with a finger as seen below in Fig. 15a. The most prominent characteristic of the shell, its toughness, is clearly compromised. Thus the findings of Li *et al.* [42] of toughening *via* micro-crack deflection within and among the nanograins of the tiles, although undoubtedly correct, needs to be augmented by consideration of the specific role of the tile's biopolymer content. At the scale of a tile lamina, reduced toughness is due to the removal of protein in the *it* regions, Fig. 14b, which permits crack propagation across lamina by the separation of tiles along their boundaries, as seen in Fig. 15b. Within single tiles, the burning off of protein leaves cavities across which cracks can propagate (*via* micro-void coalescence) as evidenced in Fig. 15b. Topographic scans of the surface of nanoindentations show that the

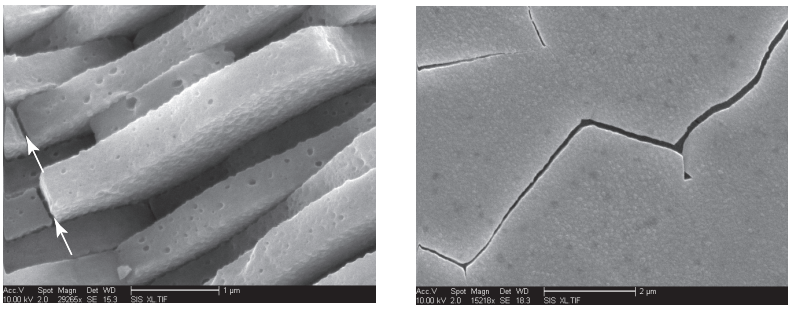

Figure 14: Heat treated nacre. (a) SEM image of heat treated nacre taken from a fractured shell fragment. Note the absence of the *it* matrix as indicated by the white arrows. (b) SEM image of a polished shell section taken parallel to the plane of the tiles. Again the removal of the *it* matrix is evident.

material crushes under the indenter tip leaving no pileup behind, in contrast to the pile-up seen in dry nacre. The lack of pile up may be attributed to cavities in heat treated tiles, which collapse under the indenter tip, thus preventing the upward flow of material. The reduced hardness can be attributed to the same phenomena. AFM topographs (not shown), that indicate height profiles, also confirm that no pileups are formed (see Huang and Li, [32]).

Relaxation is significantly less in heat treated nacre. We speculate that this is the case for two reasons: 1) the samples are completely dry after heat treatment, and 2) the main contributor to the viscoelastic response, protein,

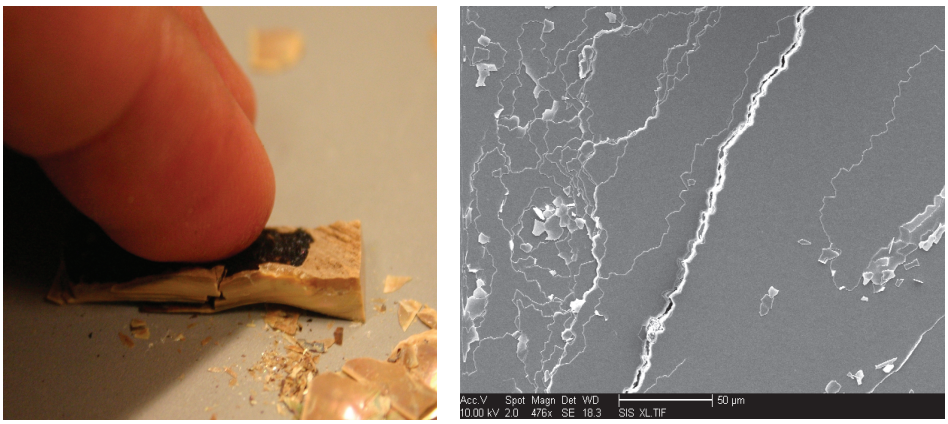

Figure 15: Heat treated nacre. (a) Photo of the easy fracture of nacre caused by a slight pressure applied by a finger. (b) SEM image of fractured heat treated nacre indicating crack propagation *via* microvoid coalescence.

has been entirely burnt off leaving only a dry chitin framework seen as sheets in Fig. 16a. The chitin network , *i.e.* the core of the *il* layers as described by Bezares *et al.* [30], that is responsible for the stiffness of the *il* and *it* matrix is most clearly revealed after treating the bioploymer matrix after demineralization *via* exposure to alkaline peroxidase followed by digestion with proteinase K. The protocols for these treatments are described in detail in Bezares *et al.* [30]. Figure 16b is an image of such network after these treatments that shows the chitin fibrils. Fibrils are generally 6-10 nm in diameter as described by Bezares *et al.* [30]. The long-term viscoelastic response is essentially entirely gone due to these same reasons; in particular the protein in the biopolymer which is responsible for the time dependent response, is gone. Calcofluor white staining (images not shown) of the sheets remaining after heat treatment verified that indeed the material was chitin. This is to be expected considering that the biopolymer framework consists entirely of protein and chitin.

It has been noted by Huang and Li [32] that heat treatment of nacre does not affect the mineral itself, and it is well documented that it is not until 400°C that aragonite undergoes a phase transformation to calcite [55]. The time dependent response of aragonite is purely a viscoplastic response, and it is more pronounced than that in heat treated nacre as seen in Fig. 7. However these results are not in conflict as we emphasize that the constitutions of the two ma-

terials are very different. In aragonite plastic flow is clear from the indentation profile in Fig. 5d which shows piling up, slip bands, and the associated load plateaus as seen in Fig. 2d. In contrast, indented heat treated nacre does not exhibit any of these characteristics associated with crystal plasticity, but rather results in indent profiles with no pileup as seen in Fig 13b. In addition, we find that the hardness of nacre is quite different than that of monolithic aragonite as seen in Fig. 16c where hardness *vs.* indentation depth is plotted for monolithic agaronite, *wet* and *dry nacre*, as well as heat treated nacre. One conclusion

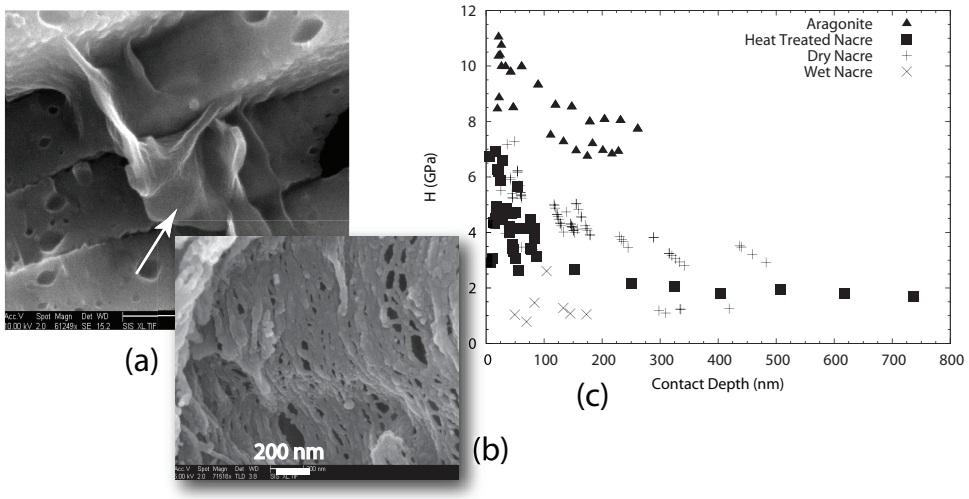

Figure 16: Heat treated nacre. (a) SEM image illustrating that after heat treatment there are residual sheets of chitin remaining within the tiles (see white arrow). (b) SEM image showing chitin firbils after treating demineralized *il* and *it* layers with alkaline peroxidase plus proteinase K. (c) Plots of hardness *vs.* indentation depth for *dry nacre*, *wet nacre*, aragonite and heat treated nacre
.

to be extracted from these observations is that monolithic aragonite is not a representative model for the tiles in nacre as has been so often assumed in the literature. Our paradigm states that a major contributing reason for nacre's excellent mechanical response is that the tiles themselves are highly toughened ceramics and not to be thought of as fragile monolithic $CaCO_3$. This coupled to the biopolymer matrix, itself a viscoelastic material with a strain to failure of $\sim 3-4\%$, leads to the observed mechanical performance. This perspective concerning the constituency of nacre is necessary *vis-à-vis* future attempts at

bio-duplication of new synthetic composites inspired by biological materials.

Acknowledgements

We also thank the staff at Hysitron, Inc. for their many helpful comments throughout this study. This study was partially supported by the US National Science Foundation under grant CMMI-0758561.

References

[1] Vincent, J.F.V. 1982, *Structural Biomaterials*, Halsted Press, New York.

[2] Sarikaya, M., Liu, J., Aksay, I.A. 1995. Nacre: Properties, crystallography, morphology, and formation. In: Sarikaya, M., Aksay, I.A. (Eds.), Biomimetics: Design and Processing of Materials, American Institute of Physics, Woodbury, New York, pp. 35-90.

[3] Evans, A.G., Suo, Z., Wang, R.Z., Aksay, I.A., He, M.Y., Hutchinson, J.W., 2001. Model for the robust mechanical behavior of nacre. J. Mater. Res. 16, 2475-2484.

[4] Munch, E., M.E. Launey, D.H. Alsem, E. Saiz, A.P. Tomsia, and R.O. Richie 2008. Tough, bio-inspired hybrid materials, Science 322, 1516-1520.

[5] Oaki, Y. and Imai, H. 2005. The hierarchical architecture of nacre and its mimetic material. Angew. Chem. Int. Ed. 44, 6571-6575.

[6] Baeuerlein, E. 2000. *Biomineralization: from biology to biotechnology and medical application*. Wiley-VCH, New York.

[7] Feng, Q.I., F.Z. Cui, G. Pu, R.Z. Wang and H.D. Li 2000. Crystal orientation, toughening mechanisms and a mimic of nacre. Mat. Sci. Engin. C11, 19-25.

[8] Gao, H., Ji., Jager, I.L., Arzt, E., Fratzl, P. 2003. Materials become insensitive to flaws at nanoscale: lessons from Nature. PNAS 100, 5597-5600.

[9] Gao, H. 2006. Application of fracture mechanics concepts to hierarchial biomechanics of bone and bone-like materials. Int. J. Fracture 138, 101-137.

[10] Sarikaya, M., J. Liu and I.A. Aksay 1992. Nacre of abalone shell: a multifuctional nanolaminated ceramic-polymer composite material. in Case, S. *Results and problems in cell differentiation in biopolymers*. Springer Verlag Amsterdam, 1-25.

[11] Wada, K., 1968. Mechanism of growth of nacre in bivalvia. Bull. Natl. Pearl Res. Lab. 13, 1561-1596.

[12] Wada, K., 1972. Nucleation and growth of aragonite crystals in the nacre of some bivalve mollusks. Biomineralization 6, 141-151.

[13] Bevelander, G., Nakahara, H. 1969. An electron microscope study of the formation of the nacreous layer in the shell of certain bivalve mollusks. Calcif. Tissue Res. 3, 84-92.

[14] Lowenstam, H.A., Weiner, S., 1989. *On Biomineralization.* Oxford University Press, New York.

[15] Wise, S., 1970. Microarchitecture and mode of formation of nacre (mother-of-pearl) in pelecypods, gastropods, and cephalopods. Eclogae Geol. 63, 775-797.

[16] Simkiss, K. and K. Wilbur 1989. *Biomineralization, cell biology and mineral deposition.* Academic Press, San Diego.

[17] Belcher, A.M. and E.E. Gooch 2000. Protein components and inorganic structure in shell nacre. in *Biomineralization.* Wiley-VCH New York 221-249.

[18] Addadi, L, D. Joester, F. Nedelman and S. Weiner 2006. Mollusk shell formation: a sourse of new concepts for understanding biomineralization processes. Chem. Eur. J. 12, 980-987.

[19] Zolotoyabko, E., Quintana, J.P., 2003. Non-destructive microstructural analysis with depth resolution. Nucl. Instr. and Meth. B 200, 382-389.

[20] Checa, A.G., Rodriguez-Navarro, A.B., 2005. Self-organization of nacre in the shells of *Pterioida* (Bivalvia: Mollusca). Biomaterials 26, 1071-1079.

[21] Cartwright, J.H.E and Checa, A.G. 2006. The dynamics of nacre self-assembly. J. R. Soc. Interface 4, 491-504.

[22] Zaremba, C.M., Belcher, A.M., Fritz, M., Li, Y., Mann, S., Hansma, P.K., Morse, D.E., Speck, J.S., Stucky, G.D. 1996. Critical transitions in the biomineralization of abalone shells and flat pearls. Chem. Mater. 8(3), 679-690.

[23] Song, F., A.K. Soh and Y.L. Bai 2003. Structural and mechanical properties of the organic matrix layers of nacre. Biomaterials 24, 3623-3631.

[24] Crenshaw, M.A. 1972. The soluble matrix of *Mercenaria mercenaria* shell. Biomineral Res. Rep. 6, 6-11.

[25] Crenshaw, M.A., Ristedt, H. 1976. The histochemical localization of reactive groups in septal nacre from *Nautilus pompilius.* In: Omori, M., Watabe, N. (Eds.) The Mechanisms of Biomineralization in Animals and Plants. Tokai University Press, Toyko.

[26] Nudelman, F., Gotliv, B.A., Addadi, L. and Weiner, S. 2006. Mollusk shell formation: Mapping the distribution of organic matrix components underlying a single aragonite tablet in nacre. J. Struct. Biol. 153, 176-187.

[27] Bezares, J., Asaro, R.J. and Hawley, M. 2008, Macromolecular structure of the organic framework of nacre in *Haliotis rufescens*: Implications for growth and mechanical behavior. J. Struct. Biol. 163, 61-75.

[28] Rousseau, M, Lopez, E., Stempflé, P, Brendlé, M., Franke, L., Guette, A., Naslain, R. and Bourrat, X. 2005. Multiscale structure of sheet nacre. Biomaterials 26, 6254-6262.

[29] Watabe, N. 1963. Decalcification of thin sections for electron microscope studies of crystal-matrix relationship in mollusk shells. J, Cell. Biol. 18, 701-702.

[30] Bezares, J., Asaro, R.J. and Hawley, M. 2010, Macromolecular Structure of the Organic Framework of Nacre in *Haliotis rufescens*: Implications for mechanical response. J. Struct. Biol. 170, pp. 484-500.

[31] Bruet, B.J.F, Qi, H.J., Boyce, M.C., Panas, R., Tai, K., Frick, L. and Ortiz, C. 2005, Nanoscale morphology and indentation of individual nacre tablets from the gastropod mollusk *Trochus niloticus*. J. Mater. Res. 20, 2400-2419.

[32] Huang, Z. and Li, X. 2009. Nanoscale structural and mechanical characterization of heat treated nacre. Mater. Sci. Eng. 29, 1803-1807.

[33] Ghosh, P., Mohanty, B., Verma, D., Katti, K.S., and Katti, D.R. 2006. - Mechanical Properties of Biological nanocomposite nacre: Multiscale modeling and experiments on nacre from red abalone. MRS Symposium Proc, Paper # 0898-L02-03.

[34] Curry, J.D. 1977. Mechanical perperties of mother of pearl in tension. Proc. R. Soc Lond B 196, 443-463.

[35] Kearney, C., Zhao, Z., Bruet, B.J.F., Radovitzky, R., Boyce, M.C. and Ortiz, C. 2006. Nanoscale anisotropic plastic deformation in single crystal aragonite. Phys. Rev. Lett. 96, 255505-1 - 255505-5.

[36] Mohanty, B., K.S. Katti and D.R. Katti 2008, Experimental investigation of nanomechanics of the mineral-protein interface in nacre. Mech. Res. Comm. 35, 17-23.

[37] Mohanty, B., Verma, D., Katti, K.S. and Katti, D.R. 2007. Time dependent nanomechanical response on nacre. Mater. Res. Soc. Proc. 975, 0975-DD03-03 - 0975-DD03-08.

[38] Shen, X., A.M. Blecher, P.K. Hasma, G.D. Stuky, and D.E. Morse 1997. ¡olecular cloning and characterization of lustrin A, a matrix protein from shell and pearl of Haliotis rufescens. J. Bio. Chem. 272, 32472.

[39] Barthelat, F. and Espinosa, H.D. 2003. Elastic properties of nacre aragonite tablets. Proc. Annual Conference and Exposition on Experimental and Applied Mechanics paper 187.

[40] Barthelat, F., Espinosa, H.D., 2005. Mechanical properties of nacre constituents: an inverse method approach. MRS Symp Proc. 844.

[41] Barthelat, F., Li, C.M., Comi, C. and Espinosa, H.D. 2006. Mechanical properties of nacre and their impact on mechanical performance. J. Mater. Res. 21, 1977-1986.

[42] Li, X., Chang, W.C., Chao, Y.J., Wang, R. and Chang, M. 2004. Nanoscale structural and mechanical characterization of a natural nanocomposite material: the shell of red abalone. Nano Lett. 4, 613-617.

[43] Smith, B.L., T.E. Schaffer, M. Viani, J.B. Thompson, N.A. Frederick, J. Kindt, A. Belcher, G.D. Stucky, D.E. Morse and P.K. Hasma 1999. Molecular mechanistic origin of the toughness of natural fibres and composites. Nature Lett. 399, 761-763.

[44] Hearmon, F.S. 1946. *The elastic constants of anisotropic materials*. Rev. Mod. Phys. 18, 409.

[45] Rief, M., M. Gautel, F. Oesterhelt, J.M. Fernandez and H.E. Gaub 1997. reversible unfolding of individual titin immunoglobulin dimains by AFM. Science 276, 1109-1112.

[46] Rief, M., J. Pascual, M. Saraste, and H.E. Gaub 1999. Single molecule force spectroscopy of spectrin repeats: low unfolding forces in helix bundles. J. Mol. Biol. 286, 553-561.

[47] Law, R., P. Carl, S. Harper, P. Dalhaimer, D.W. Specicher, and D.E. Discher 2003. Cooperativity in forced unfolding of tandem spectrin repeats. Biophys. J. 84, 533-544.

[48] Liphardt, J., B. Onoa, S.B. Smith, I. Tinoco, and C. Bustamonte 2001. reversible unfolding of single RNA molecules by mechanical force. Science 292, 733-737.

[49] Peirce, D., Asaro, R.J. and Needleman, A. 1983, Material rate dependence and localized deformation in crystalline solids. Acta metall. 31, 1951-1976.

[50] Oliver, W.C., G.M. Pharr, 2004. Measurement of hardness and elastic modulus by instrumented indentation: Advances in understanding and refinements to methodology. J. Mater. Res. 19, 3-20.

[51] Perzyna, A. 1971 *Thermodynamic Theory of Viscoplasticity*, Advances in Applied Mechanics. 11 Academic Press, New York.

[52] Mulford, R.N., R.J. Asaro and R.J. Sebring 2004. Spherical indentation of ductile power law materials, J. Mater. Res. 19, 2641-2649.

[53] Asaro, R. J. and V. Lubarda 2006, *Mechanics of Solids and Materials*, Cambridge Univ. Press, New York.

[54] Wang, R.Z., Suo, Z., Evans, A.G., Yao, N., Aksay, I.A., 2001. Deformation mechanisms in nacre. J. Mater. Res. 16, 2485-2493.

[55] Faust, G.T., 1950, Thermal analysis studies on carbonates. I. Aragonite and calcite: Am. Mineralogist, vol. 35, p. 207-224.

Submitted on February 2011

Makromolekularna struktura i viskoelastični odgovor organskog okvira sedefa u *Haliotis rufescens*: jedna perspektiva i pregled

Ispitivanje nanozasecanjem sedefa dobijenog iz ljuski *Haliotis rufescens* je pokazalo da sedef pokazuje spregnuti viskoplastično-viskoelastičan vremenski zavisan odgovor. Pored toga, nadjeno je da vlaga/sadržaj vode u sedefu doprinosi vremenski zavisnom ponašanju i ukupnih mehaničkih osobina. Detaljne simulacije konačnim elementima dozvoljavaju odredjivanje konstitutivnih parametara korišćenih za kalibraciju specifičnih vremenski zavisnih modela koji su, zatim, uporedjeni sa onim nadjenim nezavisnim merenjima kako su prikazani u literaturi.

Rezultati dovode do nove paradigme ponašanja za atraktivne strukturne kompozite i, na taj način, putevima ka potencijalno novim biomimeticima.

doi:10.2298/TAM1102075B Math.Subj.Class.: 74L15; 74C10; 74A40; 82D80.